Sine, S., & Taylor, P. (1980) *J. Biol. Chem. 255*, 10144–10156.
Sine, S. M., & Taylor, P. (1981) *J. Biol. Chem. 256*, 6692–6699.
Tsetlin, V. I. (1985) in *Peptides, Structure and Function* (Deber, C. M., Hruby, V. J., & Kopple, K. D., Eds.) pp 833–842, Pierce Chemical Co., Rockville, IL.
Walker, J. W., Richardson, C. A., & McNamee, M. G. (1984) *Biochemistry 23*, 2329–2338.
Wang, G. K., & Schmidt, J. (1980) *J. Biol. Chem. 255*, 11156–11162.
Watters, D., & Maelicke, A. (1983) *Biochemistry 22*, 1811–1819.
Weiland, G., & Taylor, P. (1979) *Mol. Pharmacol. 15*, 197–212.
Weill, C. L., McNamee, M. G., & Karlin, A. (1974) *Biochem. Biophys. Res. Commun. 61*, 997–1003.
Whiting, P., Vincent, A., & Newsom-Davis, J. (1985) *Eur. J. Biochem. 150*, 533–539.
Wolosin, J. M., Lyddiatt, A., Dolly, J. O., & Barnard, E. A. (1980) *Eur. J. Biochem. 109*, 495–505.
Wonnacott, S., Harrison, R., & Lunt, G. G. (1980) *Life Sci. 27*, 1769–1775.
Yamaoka, K., Tanigawara, Y., Nakagawa, T., & Uno, T. (1981) *J. Pharmacobio-Dyn. 4*, 879–885.

Interaction of Synthetic Analogues of Distamycin with Poly(dA-dT): Role of the Conjugated *N*-Methylpyrrole System†

Dipak Dasgupta,‡ Pradipkumar Parrack, and V. Sasisekharan*
Molecular Biophysics Unit, Indian Institute of Science, Bangalore 560 012, India
Received October 20, 1986; Revised Manuscript Received May 20, 1987

ABSTRACT: Two synthetic analogues of distamycin (Dst), PPA and PAP, containing a saturated β-alanine moiety substituting for an *N*-methylpyrrole chromophore were studied for their interactions with the double-stranded alternating copolymer poly(dA-dT)·poly(dA-dT) [abbreviated as poly(dA-dT)], with UV absorption and circular dichroism (CD) spectroscopy. The distinctive feature of these analogues is the difference in the extents of extended conjugation due to contiguous pyrrole rings: it decreases in the order Dst > PPA > PAP. Both these analogues bind to poly(dA-dT) in a way similar to Dst, as suggested from the observed red shift in the UV spectra of the ligands upon complexation and the appearance of induced Cotton effects (in the 290–350-nm region) in the CD spectra of the complexes. A comparative study of (i) the spectral features of the complexes between these ligands, Dst and netrospin (Nt) and poly(dA-dT), and (ii) the binding parameters for the association with the polynucleotide suggests that the number and relative positions of the pyrrole moieties influence the spectral features and thermodynamic stabilities of the complexes, and the latter show a progressive decrease in the order Dst > Nt > PPA > PAP. Implications of these results vis-ā-vis the molecular basis of Dst–DNA interaction are discussed.

The oligopeptide antibiotics distamycin (Dst) and netrospin (Nt) (Figure 1) bind specifically to the AT-rich regions of B-DNA structure via the minor groove in a nonintercalative fashion (Zimmer, 1975; Zimmer & Wahnert, 1986). X-ray crystallographic studies (Berman et al., 1979; Kopka et al., 1985), various physicochemical studies in solution (Zimmer & Wahnert, 1986; Wartell et al., 1974; Luck et al., 1974; Kolchinskii et al., 1975), and model building studies (Berman et al., 1979; Wartell et al., 1974; Zasedatelev et al., 1978) have indicated that the above specificity for the B-DNA conformation at AT base pairs originates from the following noncovalent interactions: (a) favorable van der Waals contacts in the minor groove of B-DNA, (b) hydrogen-bond formation between amide NH groups of the ligands and adenine N3 and/or thymine O2 atoms in the minor groove of DNA, and (c) electrostatic interactions between the phosphate backbone of DNA and positively charged terminal groups of the antibiotics. The bow-shaped structures with curved backbones for these molecules facilitate the van der Waals contacts and the hydrogen-bond formation involving the NH groups whose H atoms lie on the concave side of the molecule and point toward the bases A and T in the minor groove (Berman et al., 1979; Kopka et al., 1985). Studies on the interaction of several analogues of Dst and Nt with natural and synthetic DNAs (Zimmer & Wahnert, 1986; Lown et al., 1986) also have supported the above observations.

These studies, however, have not attempted to explain the possible role of the consecutive *N*-methylpyrrole groups (a necessary constituent of the above ligands) in the observed specific binding to DNA. On the other hand, there have also been reports of compounds (Luck et al., 1984; Zimmer et al., 1984) lacking a curved backbone, as in Nt and Dst, or potential hydrogen-bonding sites (Zakrzewska et al., 1983) exhibiting a preference for AT sequences.

In our laboratory, we have undertaken the synthesis and comparative studies of the DNA-binding and antibiotic properties of a series of compounds analogous to Dst and Nt with a view to understanding the conformational and chemical basis of their specific interactions with DNA. In a previous paper we reported the features of interactions of a Dst analogue

†This work was supported by Grant DST/MBU/VS/44 from the Department of Science and Technology, Government of India, and by Grant ICMR/MBU/VS/24 from the Indian Council of Medical Research. D.D. is the recipient of a research associateship from the Indian Institute of Science, Bangalore.
*Author to whom correspondence should be addressed.
‡Present address: Department of Biochemistry, Indian Institute of Science, Bangalore 560 012, India.

0006-2960/87/0426-6381$01.50/0 © 1987 American Chemical Society

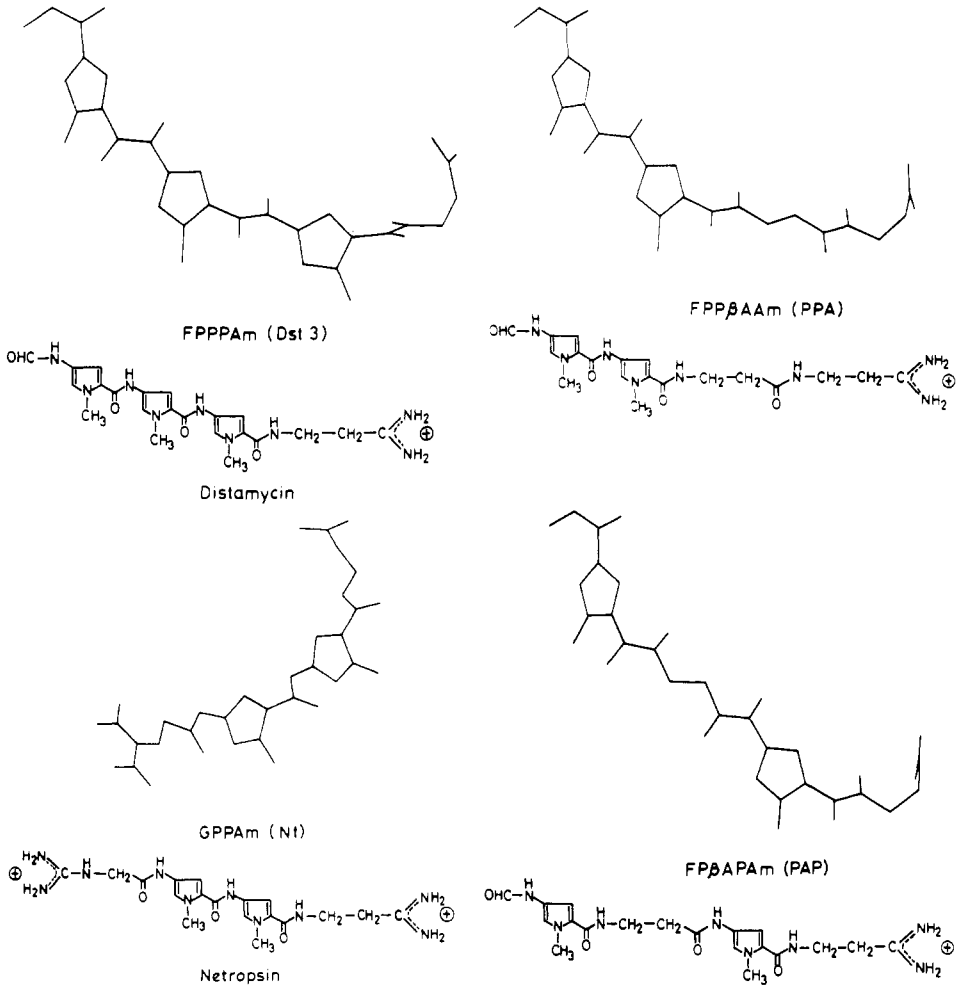

FIGURE 1: Structural formulas along with the computer-simulated backbone structures for the ligands used in this study. The formulas are abbreviated as FPPPAm and GPPAm, where F, P, G, and Am denote formyl, *N*-methylpyrrole, guanidino, and amidine groups, respectively. The synthetic analogues β-[[1-methyl-4-[1-methyl-4-(formylamino)pyrrole-2-carboxamido]pyrrole-2-carboxamido]propionamido]propionamidine and β-[1-methyl-4-[[1-methyl-4-(formylamino)pyrrole-2-carboxamido]propionamido]pyrrole-2-carboxamido]propionamidine are similarly abbreviated as FPPβAAm and FPβAPAm, where βA denotes the β-alanine moiety. For convenience, they are called PPA and PAP, respectively, in this paper. The bow-shaped backbone as found for the crystal structure of Nt was modified to obtain a structure isogeometric to B-DNA. The modified structure was used as a guideline to generate the curved backbones for Dst, PPA, and PAP.

(containing benzene rings instead of *N*-methylpyrrole) with various DNAs (Dasgupta et al., 1986). The major objective of the present study is to examine the role of extensive delocalization of the electron density via the presence of consecutive *N*-methylpyrrolecarboxamide units in the stability of the Dst–DNA complex. In order to achieve this objective, two structural analogues of Dst have been synthesized. The distinctive feature of these analogues is the replacement of a terminal and middle *N*-methylpyrrole ring of Dst by a saturated β-alanine moiety, respectively (Figure 1). Such replacement does neither significantly alter the backbone curvature of the ligand nor apparently change the distances between potential hydrogen-bonding sites in the amide residues. Thus, these analogues, PPA and PAP (see Figure 1), represent appropriate model systems for examination of the role of the *N*-methylpyrrole rings. In this paper, investigations on the interactions of PPA and PAP with poly(dA-dT)·poly(dA-dT) [abbreviated as poly(dA-dT)] by UV absorption and circular dichroism (CD) spectroscopy are reported. Similar studies with Dst and Nt are also done for comparison.

The DNA chosen for the present studies is poly(dA-dT), a B-DNA polymer (under low-salt conditions) (Assa-Munt & Kearns, 1984; Gupta et al., 1983) with the simplest sequence of dinucleotide repeat units, ApT and TpA. Poly(dA-dT) is preferred to poly(dA)·poly(dT) as the model DNA polymer because varying results are there regarding the B-DNA structure of the homopolymer (Jolles et al., 1985; Zimmerman, 1982). The results of the present studies emphasise for the first time the importance of the presence of neighboring *N*-methylpyrrolecarboxamide units in stabilizing the ligand (Dst, Nt)–polynucleotide complexes. It also helps to understand the observed spectroscopic properties of the Dst– and Nt–DNA complexes originating from the extended conjugation due to the structural repetition of the *N*-methylpyrrole units.

Materials and Methods

The compounds PPA and PAP were synthesized by modifying the procedure for distamycin synthesis (Bialer et al., 1978) to include the β-alanine moiety. Hydrochloride salts of these compounds were used. Dst and Nt were gift samples from Dr. F. Arcamone, Farmitalia, Italy, and from Lederle Laboratories, respectively. Poly(dA-dT) was from Pharmacia P-L Biochemicals and was used without further purification. The stock solutions of the ligands (PPA, PAP, Dst, and Nt) were stored at −80 °C, and concentrations were determined spectrophotometrically from the following extinction coefficients (in mM^{-1}): ϵ_{303} = 34.0 (Dst), ϵ_{295} = 21.5 (Nt), ϵ_{293} = 15.4 (PPA), and ϵ_{275} = 11.4 (PAP). ϵ_{260} = 6.7 mM^{-1} was used for poly(dA-dT) (Wells et al., 1970). The purity of the ligands was checked spectrophotometrically prior to use, since aqueous

solutions of Dst and Nt have been reported to be unstable (Arcamone, 1972).

Spectrophotometric measurements were done with Beckman DU-8B and Hitachi 557 spectrophotometers. Circular dichroic spectra were recorded in a Jasco J-20C spectropolarimeter and processed with the help of a Jasco DP-500N data processor attached to the spectropolarimeter. All measurements were carried out in aqueous solutions of 20 mM NaCl (pH 7.1) at 20 °C.

Circular dichroic values were expressed as molar ellipticity $[\theta] = (\theta_{obsd} \times 100)/(lc)$, where θ_{obsd} = observed rotation, l = 0.5 cm (path length of the cuvette) and c = molar concentration of the polynucleotide in terms of nucleotide phosphate residues. Each spectrum reported here is an average of two runs.

Determination of Binding Stoichiometry. The stoichiometry of binding of the ligands with poly(dA-dT) was measured by monitoring the change in absorbance as a function of the concentration of the ligand in the presence of a fixed concentration of the polynucleotide. With the same polynucleotide concentration in both the sample and reference cuvettes, a small volume of ligand (between 5 and 20 μL) containing the same concentration of the polynucleotide was added to the sample cuvette, and the difference in the absorbances at two wavelengths λ_1 and λ_2 was plotted against the concentration of the added ligand (λ_1 and λ_2 were 305 and 312 nm for PPA, 305 and 335 nm for Dst, and 300 and 315 nm for Nt, respectively). The stoichiometry was determined from the break in the straight lines resulting from the above plot. The ratio of the concentrations of the ligand and poly(dA-dT) corresponding to the break point gives the stoichiometry value (Dasgupta & Goldberg, 1985).

Analysis of Binding Data. The binding parameters, the intrinsic binding constant K_0, and the binding stoichiometry r_b (number of ligand molecules bound per nucleotide base), were determined from the Scatchard equation on the basis of the assumption of an independent noncooperative type of binding (Scatchard, 1949):

$$r/c_f = K_0(r_b - r)$$

where $r = c_b/c_p$, c_b and c_p = concentrations of the bound ligand and the polynucleotide, respectively, and c_f = concentration of the free ligand. A plot of r/c_f against r gives a straight line with the intercept r_b on the r axis and slope $-K_0$. The experimental points were fitted by the method of least squares to get the straight line.

For the determination of c_b, the concentration of the bound ligand, a small aliquot (between 4 and 10 μL) of the ligand was added to the sample cuvette containing a fixed concentration of the polynucleotide (between 200 and 250 μM). The reference cuvette also contained the same concentration of the polynucleotide to take care of any possible contribution to absorbance from the polynucleotide at the monitoring wavelength. However, it was so chosen that at this wavelength there is maximum change in absorbance of the ligand due to its binding to the polynucleotide and there is no (or very little) contribution from the absorbance by the polynucleotide. The concentration of the bound ligand, c_b, corresponding to each point of the titration was calculated from the relation

$$c_b = (A_f - A_b)/(\epsilon_f - \epsilon_b)$$

where A_f = absorbance of the free ligand, A_b = absorbance of the same concentration of the ligand in the presence of the polynucleotide, ϵ_f = molar extinction coefficient for the free ligand, and ϵ_b = molar extinction coefficient for the bound ligand (determined from the extinction coefficient of the ligand in the presence of a 100-fold excess of polynucleotide).

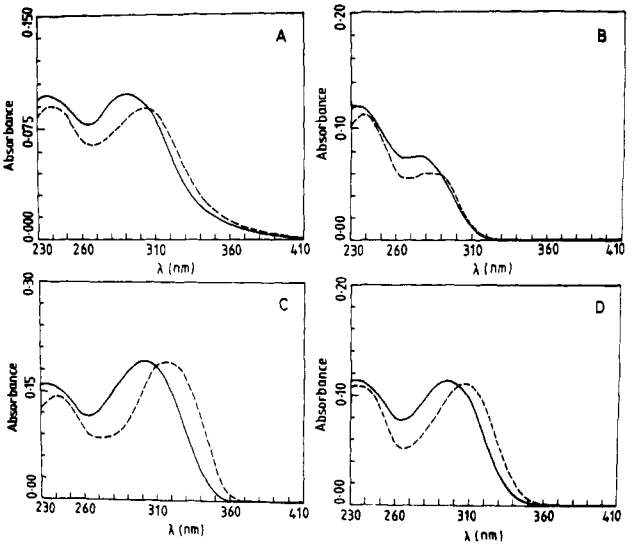

FIGURE 2: UV absorption spectra of the ligands PPA (A), PAP (B), Dst (C), and Nt (D) and their complexes with poly(dA-dT). Solid lines show the spectra of the free ligands (at a concentration of 7 μM); broken lines represent the spectra of their complexes at $r' = 0.08$, where r' is the ratio of the concentrations of the ligand and the polynucleotide. The sample and reference cuvettes contained equal concentrations of polynucleotide (87.5 μM).

Results and Discussion

Absorption Spectra of the Ligands and Their Complexes with Poly(dA-dT). Figure 2 shows the absorption spectra of the free ligands PPA, PAP, Dst, and Nt. It is apparent from the figure that the position and intensity of the long-wavelength peak depends on the number of *N*-methylpyrrole groups and their relative positions. This observation, along with the fact that the free *N*-methylpyrrole shows a peak around 245–250 nm, suggests that the long-wavelength peak arises due to the presence of more than one *N*-methylpyrrole chromopore connected by the peptide bonds. This explains the observation that there is a progressive shifting of the long-wavelength peak from 275 nm for PAP (having no contiguous *N*-methylpyrrole groups) to 303 nm for Dst (which has three contiguous *N*-methylpyrrole groups).

The binding of the synthetic ligands PPA and PAP to poly(dA-dT) is evident from the change in the UV absorption spectra of the free ligands in the presence of the polynucleotide. The absorption spectra of the bound PPA and PAP, along with those of the bound Dst and Nt [at the same value of r', the input ratio of the concentrations of the ligand and poly(dA-dT)], are shown in Figure 2. The salient features emerging from the comparative study of the spectra can be summarized as follows: (a) all the four ligands, PPA, PAP, Dst and Nt undergo red shifts of their absorption maxima due to complex formation with poly(dA-dT); (b) the extent of the red shift depends upon the nature of the compounds and follows the order Dst ($\Delta\lambda$ = 15–16) > Nt ($\Delta\lambda$ = 12) = PPA ($\Delta\lambda$ = 11) > PAP ($\Delta\lambda$ = 5), where $\Delta\lambda$ denotes the value of the red shift in nanometers. Both PPA and PAP exhibit isosbestic points (spectra not shown) for the complexes upto an input ratio r' = 0.1. This perhaps indicates a single mode of binding upto that ratio.

It also follows from the discussion in the preceding paragraph that the red shifts of the long-wavelength peaks in the UV absorption spectra of the ligands upon binding to poly(dA-dT) arise from the perturbation of the coupled chromophore system of the 1-methylpyrrole-2-carboxamide groups on alignment with poly(dA-dT). An extension of this expla-

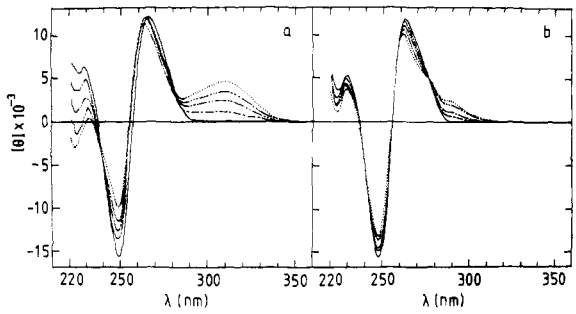

FIGURE 3: CD spectra of poly(dA-dT) (300 μM) in the presence of PPA (a) and PAP (b) at different input ratios (r') of the concentrations of the ligand and the polynucleotide: 0 (—), 0.02 (– – –), 0.04 (– · – · –), 0.06 (– · · – · · –), and 0.08 (···).

nation might lead one to suggest that the red shift in the UV absorption spectra is probably indicative of an increased delocalization of the π-electrons in the ligands as a sequel to their binding to DNA. The difference in the red shifts of the long-wavelength peaks associated with the binding of PPA and PAP to poly(dA-dT), then, suggests that the presence of an intervening β-alanine in PAP reduces such delocalization in the complex.

CD Spectra of Ligand–Polynucleotide Complexes. The binding of PPA and PAP to poly(dA-dT) was further substantiated by the appearance of an extrinsic Cotton effect (Figure 3), similar to that reported for Dst and Nt. Figure 3 shows the effect of increasing concentrations of the ligands (PPA and PAP) on the CD spectrum of a fixed concentration of the polynucleotide. As apparent from the figure, there is an increase in the intensity of the induced band above 285 nm with increasing input ratios. The CD spectra for the PAP–poly(dA-dT) complex are characterized by the presence of a shoulder around 290 nm, in contrast to a broad induced band with a maximum of 308 nm for the PPA complex. Both the synthetic ligands exhibit isosbestic points (at 282 nm for PPA and at 276 nm for PAP) upto $r' = 0.09$. This provides further evidence for a single type of complex formation for $r' < 0.01$. There is no pronounced effect on the conservative nature of the B-DNA-type spectrum of poly(dA-dT) due to the addition of the ligands—both the positive and negative peaks decrease by the same extent.

Figure 4 shows the CD spectra of poly(dA-dT) in the presence of PPA, PAP, Dst, and Nt at $r' = 0.08$. The following features are brought forth from a comparative study of the spectra: (i) the conservative B-DNA-type spectrum in the region 230–280 nm is maintained in the complexes for all the four ligands; (ii) the spectra of the complexes cross the free polynucleotide spectrum at different wavelengths, depending upon the ligand; (iii) the peak positions of the induced bands also depend on the nature of the ligands (318 nm for Dst, 309 nm for PPA, 303 nm for Nt, and a shoulder at 290 nm for PAP); (iv) the molar ellipticity at the peak of the induced band also depends on the nature of the ligands and follows the order Dst > Nt > PPA > PAP. The induced CD band originates from the asymmetric environment of the *N*-methylpyrrole chromophores in the complex (Zimmer, 1975; Zimmer & Wahnert, 1986). Therefore, from the above observations it appears that the intensity of this band depends on the number and the relative position of the bound chromophore. The three *N*-methylpyrrole chromophores in Dst give rise to the strongest induced band. Between Nt and PPA, both containing the same number of consecutive *N*-methylpyrrole chromophores, Nt exhibits an induced band with higher molar ellipticity. This might be due to the presence of two charged terminal groups in Nt in contrast to one in PPA. The

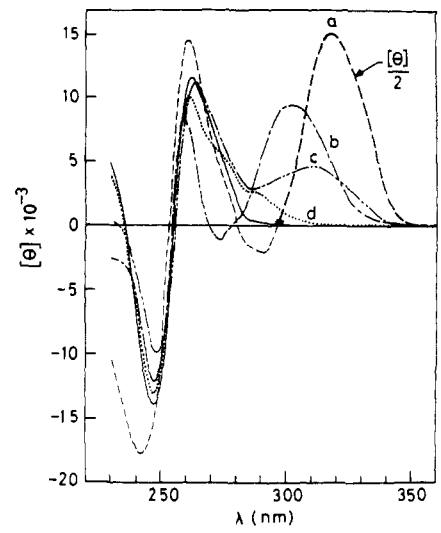

FIGURE 4: CD spectra of poly(dA-dT) alone (300 μM) (—) and in the presence of the ligands (a) Dst (– –), (b) Nt (– · –), (c) PPA (– · · –), and (d) PAP (···) at $r' = 0.08$. For Dst, the molar ellipticity in the region between 300 and 350 nm is plotted at a reduced scale as indicated with an arrow.

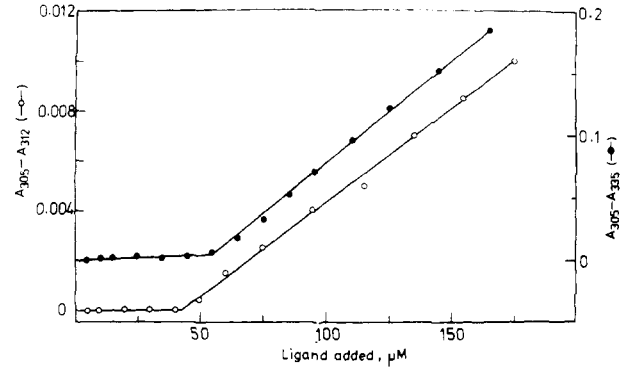

FIGURE 5: Determination of the binding stoichiometries for the ligand–poly(dA-dT) interactions. Plots of the difference in absorbances (at the wavelengths indicated by the subscripts) against the concentrations of the ligands Dst (●) and PPA (○). Concentration of poly(dA-dT) in both sample and reference cuvettes was 60 μM. r_b was calculated from the plot as described under Materials and Methods.

presence of an intervening saturated β-alanine moiety in PAP apparently leads to the absence of a peak beyond 300 nm; instead, a shoulder at 290 nm is observed.

Results of both UV absorption and CD spectroscopic studies strongly suggest that the degree of extended conjugation via the pyrrole rings and amide bonds in the ligands is different in the four ligand–polynucleotide complexes. In order to study the influence of these different degrees of conjugation, if any, on the thermodynamic stability of the complex, we have evaluated quantitatively the two binding parameters, viz., the binding stoichiometry r_b and the intrinsic binding constant K_0, which characterize a reversible interaction.

Binding Stoichiometry for Ligand–Poly(dA-dT) Complexes. The binding stoichiometries were determined from UV absorption (described under Materials and Methods) and from CD spectral titrations. Representative examples for the determination of r_b for Dst and PPA (from UV absorption) are shown in Figure 5. In the case of PPA, another break point was observed corresponding to the ratio $r_b = 0.3$ (not shown in Figure 5). This indicates the formation of a second type of complex at a higher ratio of the concentrations of PPA and poly(dA-dT).

For the determination of the binding stoichiometry from CD titrations, the molar ellipticity $[\theta]$ at the maximum of the

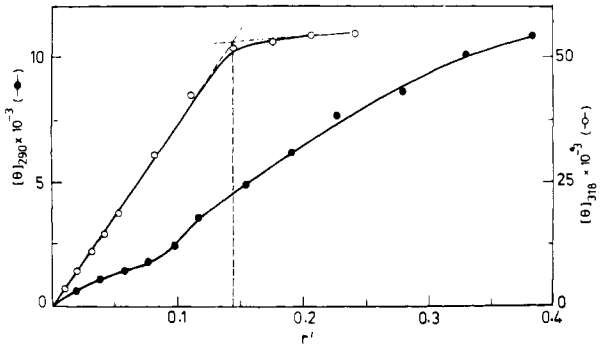

FIGURE 6: Variation of the molar ellipticity with r'. Plots of $[\theta]_{318}$ for Dst (O) and $[\theta]_{290}$ for PAP (●) against the input ratio r'. The concentration of poly(dA-dT) was 300 μM. Note the kink in the curve for PAP at $r' = 0.09$.

Table I: Stoichiometry of Binding of the Ligands to Poly(dA-dT)

ligand	stoichiometry, r_b = [ligand]/[polynucleotide]: from UV absorption[b]	from CD[c]
Dst	0.13	0.14
Nt	0.14	0.12
PPA	0.10	0.09
PAP		0.09

[a] Terms in square brackets denote the concentrations in moles per liter. [b] As found from the break point in the plot of the difference in absorbances (at two wavelengths) against the concentration of the ligand added, such as shown in Figure 5. [c] From CD titration curves, such as shown in Figure 6.

induced band was plotted against the input ratio r'. Figure 6 illustrates how the binding stoichiometry for Dst–poly(dA-dT) was calculated; the value was in good agreement with the r_b value found from UV titration. The titration curves for PPA and Nt, however, do not exhibit a plateau; instead, they show a kink at the value of $r' = r_b$ (where r_b = binding stoichiometry from UV absorption data). This phenomenon, earlier reported for the Nt–poly(dA-dT) complex (Burckhardt et al., 1985), arises due to two modes of binding of these ligands to poly(dA-dT). The r' values at the kink correspond to the binding stoichiometry for the first (stronger) mode of binding. The r_b values, thus calculated for all the ligands, are summarized in Table I. The values determined by the two methods are in good agreement.

Such an agreement led us to determine the r_b value for PAP by CD titration. As apparent from the UV absorption spectra of PAP and its complex with poly(dA-dT) (Figure 2B), the binding stoichiometry could not be determined by UV titration. Figure 6 shows the CD titration curve for PAP. This curve is also indicative of two modes of binding (Burckhardt et al., 1985); the binding stoichiometry for the first mode is determined from the position of the kink.

Table I shows that the replacement of an *N*-methylpyrrole of Dst by a β-alanine, as in PPA and PAP, decreases the binding stoichiometry. Nt shows a stoichiometry higher than that for PPA—this can be attributed to the shorter end to end distance for Nt.

Binding Constant for Ligand–Poly(dA-dT) Interactions. There is a good correlation between the binding stoichiometry values determined above and those evaluated from the Scatchard plots. In case of all the ligands, their interactions with poly(dA-dT) could be described by Scatchard plots, thereby supporting an independent noncooperative type of binding for them. Figure 7 shows the representative plots for PPA and Dst. The plot over the entire range of values of r for the PPA–poly(dA-dT) interaction is shown in the inset. The biphasic plot indicates the presence of two types of binding

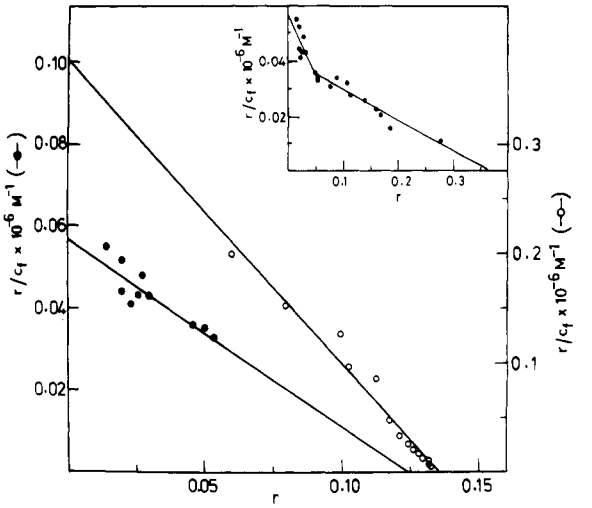

FIGURE 7: Determination of intrinsic binding constant K_0 and binding stoichiometry r_b for the ligand–polynucleotide interactions. Scatchard plots of r/c_f against r for Dst (O) and PPA (●). Inset shows the plot for PPA over the entire range of values of r.

Table II: Binding Parameters for Ligand–Poly(dA-dT) Interaction[a]

ligand	monitoring wavelength[b] (nm)	K_0 (M^{-1})	r_b	K_a ($=K_0 r_b$) (M^{-1})
Dst	330	2.8×10^6	0.14 (0.13)[c]	3.8×10^5
Nt	320	2.0×10^6	0.13 (0.14)[c]	2.6×10^5
PPA	320	4.6×10^5	0.12 (0.10)[c]	5.7×10^4
PAP	280	0.8×10^5	0.085 (0.09)[d]	6.8×10^3
PAP	290			(8.4×10^3)[e]

[a] Determined from the Scatchard plots as shown in Figure 7. For the biphasic plots, the values quoted are for the first mode of binding. [b] Denotes the wavelength at which the absorbance change was measured to determine c_b. [c] Values taken from Table I, UV titration. [d] From Table I, CD titration. [e] Determined by CD as mentioned in the text.

sites. This is in accordance with the observation that a single isosbestic point is absent in the UV and CD spectra of PPA–poly(dA-dT) complexes over $0.1 \leq r' \leq 0.3$ (spectra not shown). The second (weaker) mode of binding is currently being investigated. In the present case, it is worth mentioning that Dst, in contrast to PPA and PAP, shows a single mode of binding. The relevant binding affinities are summarized in Table II. It may be pointed out that the determination of c_b for the construction of the Scatchard plot for PAP was done at 280 nm, a wavelength where there is a contribution in the absorbance from poly(dA-dT). This was taken care of by adding an equal concentration of poly(dA-dT) to the reference cuvette—the linearity of the Scatchard plot supports the validity of the method. The excellent agreement of the r_b values from the Scatchard method and CD titration lends further support. In the case of PAP, the apparent binding constant K_a ($=K_0 r_b$) was also evaluated by means of CD spectroscopy, employing the fact that the free ligand does not have any CD band in the nonabsorbing region of poly(dA-dT). The knowledge of $[\theta]$ under the condition of an excess concentration of poly(dA-dT), when PAP can be assumed to be bound completely, enabled us to determine c_b corresponding to any point of the titration from the relation $c_b = a[\theta]_{obsd}/[\theta]_0$, where a denotes the concentration of PAP and $[\theta]_0$ and $[\theta]_{obsd}$ denote the ellipticities for PAP in the totally bound state and at any point of the titration, respectively. K_a was calculated from the equation $K_a = c_b/[(a - c_b)(b - c_b)]$, where b = concentration of poly(dA-dT). $[\theta]_0$ was calculated at 290 nm

Table III: Free Energy for Ligand–Poly(dA-dT) Interactions[a]

ligand	ΔF (kcal/mol)	ligand	ΔF (kcal/mol)
Dst	−7.4	PPA	−6.35
Nt	−7.2	PAP	−5.1

[a] Calculated from the relation $\Delta F = -RT \ln K_a$. Values of K_a taken from Table II; $T = 293$ K.

from the observed ellipticity θ at $r' = 0.02$ from the relation $[\theta]_0 = (\theta \times 100)/0.5a$. $[\theta]_{obsd}$ was calculated similarly for $r' = 0.06$. K_a calculated by this method agrees reasonably well with that determined from the Scatchard plot (Table II). The binding constants for the interactions between Dst and Nt with poly(dA-dT) agree with those reported earlier (Zimmer & Wahnert, 1986). We could not however find any binding site with an affinity of the order of 10^8 M^{-1} for Nt (Luck et al., 1974). This may be due to the limitation of the methodology used by us.

Table II clearly suggests that the binding affinity depends on the number and the relative positions of the *N*-methylpyrrole groups. It follows the order Dst > Nt > PPA > PAP. The value of the binding constant for Nt is higher compared to that for PPA, though both of them contain two *N*-methylpyrrole moieties in a contiguous position. This apparent anomaly can be easily ascribed to the fact that Nt possesses two positive charges at either end, which increases its potential for making an additional electrostatic interaction with the phosphate backbone compared to PPA. The trend is, otherwise, as expected; and it emphasizes the role of consecutive *N*-methylpyrrole groups in imparting stability to the complex. Between PPA and PAP, the presence of an intervening β-alanine moiety between two *N*-methylpyrrole units has reduced the DNA-binding affinity of PAP. The decrease in affinity may also be partly due to the difference in van der Waals contacts.

Role of N-Methylpyrrole Groups in the Interaction. Comparative studies of the spectroscopic characteristics of the complexes of the four ligands with poly(dA-dT), a model B-DNA, and the evaluation of their binding affinities bring home the important aspect of the hitherto unnoticed role of chromophoric *N*-methylpyrrole moieties in the Dst (and Nt)–DNA interaction. Independent UV absorption and CD spectroscopic studies on the interaction of PPA and PAP with several natural and synthetic DNAs have shown that the replacement of an *N*-methylpyrrole chromophore of Dst by a β-alanine moiety (as in these ligands) does not affect their minor groove binding and AT base specific nature (Parrack et al., 1987). However, the present studies demonstrate that, concomitant with the increase in the number of contiguous pyrrole chromophores from Dst to PAP via PPA, there is a progressive change in the spectroscopic properties (such as decrease in the extent of red shift in the UV spectra and in the strengths of the induced bands in the CD spectra) of the ligand–DNA complexes. One might suggest from these observations that the extensive delocalization (of the π-electrons of the chromophoric *N*-methylpyrroles via the intervening unsaturated amide bonds) plays a significant role in giving rise to the above spectroscopic features of the ligand–DNA complexes. On the other hand, results presented in Tables II and III clearly indicate that the affinity of the ligands for poly(dA-dT) decreases progressively as the number of adjacent pyrrole moieties is decreased. It can, therefore, be proposed that the extended conjugation via adacent pyrrole units in Dst/Nt imparts stability to their complexes with DNA and contributes to the free energy of binding but does not play a significant role in the AT-specific nature of the interaction.

Acknowledgments

We are grateful to Dr. Jayalekshmy Ayyer for her involvement in designing and carrying out the chemical syntheses of the reported analogues and also in their purification and characterization. We thank the IDL Nitro Nobel Basic Research Institute, Bangalore, for use of the Hitachi 557 spectrophotometer and Rajani Srinivasan for assistance in using the Beckman DU-8B spectrophotometer.

Registry No. Dst, 39389-47-4; PPA, 108260-33-9; PAP, 108260-34-0; Nt, 1438-30-8; poly(dA-dT), 26966-61-0.

References

Arcamone, F. (1972) in *Medicinal Chemistry*, Pratesi, P., Ed., pp 29–45, Butterworth, London.

Assa-Munt, N., & Kearns, D. R. (1984) *Biochemistry 23*, 691–697.

Berman, H., Neidle, S., Zimmer, C., & Thrum, H. (1979) *Biochim. Biophys. Acta 561*, 124–131.

Bialer, M., Yagen, B., & Mechoulam, R. (1978) *Tetrahedron 34*, 2389–2391.

Burckhardt, G., Votavova, H., Sponar, J., Luck, G., & Zimmer, C. (1985) *J. Biomol. Struct. Dyn. 2*, 721–736.

Dasgupta, D., & Goldberg, I. H. (1985) *Biochemistry 24*, 6913–6920.

Dasgupta, D., Rajagopalan, M., & Sasisekharan, V. (1986) *Biochem. Biophys. Res. Commun. 140*, 626–631.

Gupta, G., Sarma, M. H., Dhingra, M. M., Sarma, R. H., Rajagopalan, M., & Sasisekharan, V. (1983) *J. Biomol. Struct. Dyn. 1*, 395–416.

Jolles, B., Laigle, A., Chinsky, L., & Turpin, P. Y. (1985) *Nucleic Acids Res. 13*, 2075–2089.

Kolchinskii, A. M., Mirzabekov, A. D., Zasedatelev, A. S., Gursky, G. V., Grokhovsky, S. L., Zhuze, A. L., & Gottikh, B. P. (1975) *Mol. Biol. (Moscow) 9*, 14–20.

Kopka, M. L., Yoon, C., Goodsell, D., Pjura, P., & Dickerson, R. E. (1985) *Proc. Natl. Acad. Sci. U.S.A. 82*, 1376–1380.

Lown, J. W., Krowicky, K., Bhat, U. G., Skorobogaty, A., Ward, B., & Dabrowiak, C. (1986) *Biochemistry 25*, 7408–7416.

Luck, G., Triebel, H., Waring, M., & Zimmer, C. (1974) *Nucleic Acids Res. 1*, 503–530.

Luck, G., Zimmer, C., & Baguley, B. C. (1984) *Biochim. Biophys. Acta 782*, 41–48.

Parrack, P., Dasgupta, D., Ayyer, J., & Sasisekharan, V. (1987) *FEBS Lett. 212*, 297–301.

Scatchard, G. (1949) *Ann. N.Y. Acad. Sci. 51*, 660–663.

Wartell, R. M., Larson, J. E., & Wells, R. D. (1974) *J. Biol. Chem. 249*, 6719–6731.

Wells, R. D., Larson, J. E., Grant, R. C., Shortle, B. E., & Cantor, C. R. (1970) *J. Mol. Biol. 54*, 465–497.

Zakrzewska, K., Lavery, R., & Pullman, B. (1983) *Nucleic Acids Res. 11*, 8825–8839.

Zasedatelev, A. S., Zhuze, A. L., Zimmer, C., Grokhovsky, S. L., Tumanyan, V. G., Gursky, G. V., & Gottikh, B. P. (1978) *Stud. Biophys. 67*, 47–48.

Zimmer, C. (1975) *Prog. Nucleic Acid Res. Mol. Biol. 15*, 285–318.

Zimmer, C., & Wahnert, U. (1986) *Prog. Biophys. Mol. Biol. 47*, 31–112.

Zimmer, C., Reinert, K. E., Luck, G., Wahnert, U., Lober, G., & Thrum, H. (1971) *J. Mol. Biol. 58*, 329–348.

Zimmer, C., Luck, G., & Burckhardt, G. (1984) *Stud. Biophys. 104*, 247–251.

Zimmerman, S. B. (1982) *Annu. Rev. Biochem. 51*, 395–427.